THE MODELING STUDY USING TOUGH2 AND THE MICRO-GRAVITY CHANGE IN YANAIZU-NISHIYAMA GEOTHERMAL FIELD

Kazumi Osato[*1], Tatsuya Sato[*1], and Seiichi Yokomoto[*2]

[*1]:Geothermal Energy Research and Development Co., Ltd.
11-7 Kabuto-cho, Nihonbashi, Chuo-ku, Tokyo 103, Japan
ohsato@gerd.co.jp/tatuya@gerd.co.jp

[*2]:Okuaizu Geothermal Co., Ltd.
3-2-13, Nihonbashi-honcho, Chuo-ku, Tokyo 103, Japan
oagtky@mxg.meshnet.or.jp

INTRODUCTION

In many existing geothermal power stations, history matching and numerical model review is continuously carried out, even after the start of operations, in order to optimize the numerical model of the geothermal reservoir so that steam can be generated satisfactorily and the accuracy of the production forecast can be improved. In many geothermal power stations flow data from a specific well, or even from a specific flash separator connected multiple wells in extreme cases, are mostly used for production history matching. Many geothermal power stations have some observation wells in which long-term changes in reservoir pressure are to provide data for production history matching. However, in areas where vaporization in the formation occurs, it may be difficult to measure the pressure change behavior due to vaporized areas. When a geothermal reservoir model is constructed from such poor information, it may be difficult to accurately predict the amount of production. In order to overcome such difficulties, it has been tried in actual geothermal areas to estimate the fluid behavior in a reservoir from changes in physical properties measured in surface surveys, e.g., micro-gravity surveys (Allis and Hunt, 1986; Motoyama et al., 1992; Sugihara, 1997).

This report describes the numerical modeling study using TOUGH 2 (Pruess, 1991) and a post-processor "GRAV/TOUGH2" for micro-gravity, to the Yanaizu-Nishiyama geothermal field (65MW) located in Yanaizu-cho in Fukushima Prefecture. Tohoku Electric Power Company is responsible for the power generation section of the station, and Okuaizu Geothermal Co. is responsible for the steam supply section. The station began operation in May 1995. A four-year joint study program was started in fiscal 1994 by both companies. A precision gravity survey was performed each year at 83 measuring points, including 8 benchmark points, in a 12 km^2 area for the purpose of monitoring the gravity change before and after the start of operation of the station and helping understand geothermal fluid behavior in a geothermal reservoir and how it is related to production and injection of fluid.

CONSTRUCTION OF A NUMERICAL MODEL

According to the underground temperature distribution, a range with underground temperature 200℃ or higher, which is considered to be a promising reservoir, spreads from the northeast side of the Oizawa Fault towards the southwest side of the Onogawara Fault. In the high-temperature range, which is assumed to be the center of the up-flow, lost circulation frequently occurs and feed points of production wells are scattered. It was conjectured that there exists an up-flow from an underground high-temperature area along the faults under this high temperature range, and that the convection area extends from the northeast side of the Oizawa Fault and from the southwest side of the Onogawara Fault at a width of approximately 1 km. In the numerical model, the NE-SW length of the area was taken to be 4.6 km so that the fault directions can be taken into consideration and the high temperature range can be covered. The NW-SE length was taken to be 3.2 km so that the Kitanosawa Fault and the Sudarezawa Fault, as well as the faults which are considered to restrict natural convection flow (Chinoikezawa, Sarukurazawa, Oizawa, Takiyagawa, and Onogawara Falt), can be covered. As for the internal grid, the area near the faults relating to production and injection was divided into smaller blocks and the surrounding area was divided into larger blocks. EOS2 (H_2O-CO_2) of TOUGH2 was used as the state equation to take the CO_2 of geothermal fluid into consideration.

STEADY-STATE MODELING BY MEANS OF NUMERICAL SIMULATION

Since the numerical simulation was done just before the start of operation of the station, the model was optimized according to the steady-state. However, review of the numerical model based on the production history after the start of operation has not been done. The first numerical model was constructed by the optimal model in 1988 for the steady-state simulation taking data from new wells into consideration. Figure 1 shows the underground temperature distribution calculated using the steady-state-optimized numerical simulation, the actual underground temperature distribution (both at 1,500 m below sea level) with the grids of the fourth and Figure 2 shows the NE-SW Cross-sectional view of the underground temperature distribution, lost-circulation points, feed points of production wells, and projected geological columns.

PREDICTION OF THE GRAVITY CHANGE USING THE POST-PROCESSOR

In calculating the gravity change, the Talwani method (Plouff, 1976) for estimating of anomalies in a polygonal prism with abnormal density was used.

To calculate the density change in the rocks, the porosity (ϕ), the mass percent in the vapor phase (S_g), the density in the vapor phase (δ_g), and the density in the liquid phase (δ_w) of each block rock, which are input/output values of TOUGH 2, are used. If the density change in the rocks is ignored, the density change is determined by the density change of geothermal fluid in the pores in the rock. The density of geothermal fluid in the rock density (ρ) is defined below.

$$\rho = \left[s_g \cdot \delta_g + \left(1 - s_g\right)\delta_w\right] \cdot \phi \qquad (1)$$

According to the Talwani method, the gravity change in a polygonal prism under the ground (Figure 3), ΔZ in thickness and ρ in density, is given by the following equation:

$$g = \gamma\rho S_m \sum_{i=1}^{n} \left\{ \begin{array}{l} S_p A[Z_2 - Z_1] + Z_2\left[\tan^{-1}\dfrac{Z_2 d_1}{PR_{12}} - \tan^{-1}\dfrac{Z_2 d_2}{PR_{22}}\right] \\ -Z_1\left[\tan^{-1}\dfrac{Z_1 d_1}{PR_{11}} - \tan^{-1}\dfrac{Z_1 d_2}{PR_{21}}\right] - P\ln\left[\dfrac{R_{22}+d_2}{R_{12}+d_1}\dfrac{R_{11}+d_1}{R_{21}+d_2}\right] \end{array} \right\} \qquad (2)$$

where g: gravity anomaly in the polygonal prism

γ : universal gravitation constant

ρ : density of block i

S_m=1: the case in which the height of the center of gravity is lower than the observed value

S_m=-1: the case in which the height of the center of gravity is higher than the observed value

S_p=1: the case in which P is a positive value

S_p=-1: the case in which P is a negative value

and A, d_1, d_2, P, R_{11}, R_{12}, R_{21}, and R_{22} are given as follows:

$$A = \cos^{-1}\left(\frac{X_1X_2 + Y_1Y_2}{r_1r_2}\right) = \cos^{-1}\left(\frac{X_1X_2 + Y_1Y_2}{\sqrt{X_1^2 + Y_1^2}\sqrt{X_2^2 + Y_2^2}}\right)$$

$$d_1 = X_1\frac{X_2 - X_1}{\sqrt{(X_2 - X_1)^2 + (Y_2 - Y_1)^2}} + Y_1\frac{Y_2 - Y_1}{\sqrt{(X_2 - X_1)^2 + (Y_2 - Y_1)^2}}$$

$$d_2 = X_2\frac{X_2 - X_1}{\sqrt{(X_2 - X_1)^2 + (Y_2 - Y_1)^2}} + Y_2\frac{Y_2 - Y_1}{\sqrt{(X_2 - X_1)^2 + (Y_2 - Y_1)^2}}$$

$$P = X_1\frac{Y_2 - Y_1}{\sqrt{(X_2 - X_1)^2 + (Y_2 - Y_1)^2}} - Y_1\frac{X_2 - X_1}{\sqrt{(X_2 - X_1)^2 + (Y_2 - Y_1)^2}}$$

$$R_{11} = \sqrt{X_1^2 + Y_1^2 + Z_1^2}$$

$$R_{12} = \sqrt{X_1^2 + Y_1^2 + Z_2^2}$$

$$R_{21} = \sqrt{X_2^2 + Y_2^2 + Z_1^2}$$

$$R_{22} = \sqrt{X_2^2 + Y_2^2 + Z_2^2} \qquad (3)$$

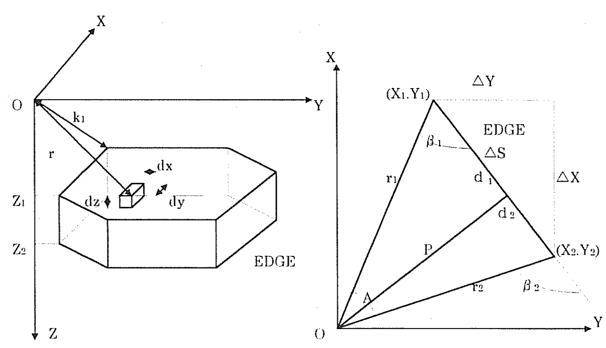

(Left) BASIC ELEMENT-POLYGONAL PRISM

(Right) PLAN VIEW OF ONE EDGE OF PRIZM

Figure 3. Prism Model Used in the Talwani Method

COMPARISON AND EXAMINATION OF REAL DATA

Figure 4 shows the gravity change due to the start of operation estimated from the differences between the data before and after the start of operation (1994 and 1995) obtained from periodic precision gravity measurements after normalizing for the effects of altitude and tide with the results of the gravity change prediction after one year of operation , traces of wells, and the fault distribution. The following facts were clarified from the figure.

(1) In comparison with the predicted values (-10 or less), a much larger negative gravity change (-60 μgal) occurred in the production zone and surrounding area. Such a large gravity change may be due to either a higher rate of vaporization in the reservoir due to less recharge than expected before the start of operation, or a higher rate of steam up-flow through the faults than that used in the numerical simulation, or both.

(2) Although the prediction gives a simple configuration of gravity changes due to the limitation of the division of blocks in the numerical modeling, according to the actual measurement, gravity changes occur according to the fault configuration which restricts the reservoir. This indicates the possibility that a steam phase is formed below the cap lock due to restriction by the faults.

(3) Also in the injection zone, a larger positive gravity change (about +several tens of μgal) was occurred, compared with the predicted value (about +several μgal).

(4) As for differences from the numerical model, since the numerical model is basically a porous model, the rate of steam up-flow was less than in the actual reservoir which is restricted by longitudinal faults. Consequently, the rate of vaporized formation along the faults below the cap lock formation in the actual reservoir was lower than assumed in the numerical model.

(5) Since the gravity value in the injection zone was increased, it may be possible that the underground water level had actually been raised. Since increased gravity values were also observed in areas surrounding the injection zone it may also be possible that the effects of the overall geological changes in the area covering the standard benchmark points are combined with those of the underground water level rise.

In 1996, the second stage of the numerical simulation has been done using the production history from the start of the plant and the production zone was divided more precisely using the location of the newest wells. The layers was also divided more precisely. Figure 5 shows the micro-gravity change after one year production that was calculated by the estimated model. We did not try to match the measurement of the micro-gravity data in this study but the shape and value of the gravity anomaly became more reasonable to the measurement than the last study. The result of calculated micro-gravity change shows the reservoir model was improved by the history matching from the start of the plant. However, the matching of the micro-gravity change is not completely and the more improvement of the numerical model study using both the production history and the micro-gravity change will be required.

CONCLUSIONS

In the above, the following facts were clarified.

(1) Comparison of the results of precision gravity measurement using the post-processor with the results of the previous numerical modeling shows that precision gravity measurement may be used in conjecturing the fine structure inside a reservoir restricted by faults. Therefore, it was proven that precision gravity measurement can be effectively used in the future review of the numerical model.

(2) Since the results of precision gravity measurements cannot explain detailed phenomena quantitatively, it will be necessary in the future to review both the details of the numerical model and to reexamine the measurement method.

ACKNOWLEDGMENT

The authors wish to thank Tohoku Electric Company and Okuaizu Geothermal Co. for their support and permission to publish this paper.

REFERENCES

Allis R. G. and Hunt, T. M. (1986), "Analysis of exploitation -Induced gravity changes at Wairakei geothermal field-", Geophysics, 51, pp.1647-1660

Motoyama, T., Ehara, S., Mogi, T. and Akasaka, C. (1992), "Reservoir monitoring by observations of gravity changes – A case history of Takigami geothermal field-", Abstracts with Programs of 1992 Annual Meeting, GRCJ, A5.

Plouff, D. (1976), "Gravity and magnetic fields of polygonal prisms and application to magnetic terrain corrections", Geophysics, 41, pp.727-741.

Pruess, K. (1991), "TOUGH2 – A General-purpose numerical simulator for multiphase fluid and heat flow.", Report LBL-29400, Lawrence Berkeley Laboratory

Sugihara, M. (1997), "Continuous Gravity Monitoring of Geothermal Activity", Proceeding of the 96th SEGJ Conference, pp.321-323.

Takasugi,S., Sato,T., and Osato,K. (1994), "Parametric Study of Gravity Change Accompanying Geothermal Reservoir Change Calculated by Numerical Simulation", Proceeding of 19th Annual Workshop on Geothermal Reservoir Engineering, Stanford Geothermal Program, pp.277-283.

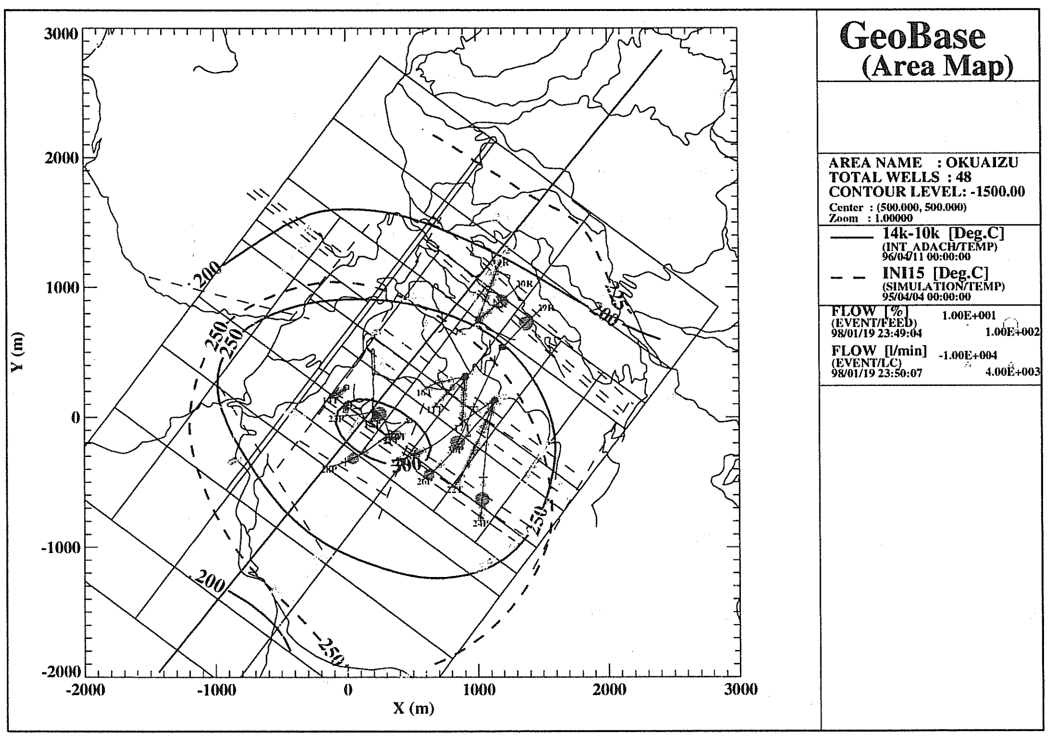

Figure 1. Calculated underground temperature distribution (1,500 m below sea level) optimized by steady-state modeling (dash line), and the actual underground temperature distribution (solid line) with grids of the fourth layer, lost-circulation points (triangle), feed points from PTS logging (circle), faults distribution (solid line) at 1,200m below sea level) and well trajectories (solid line)

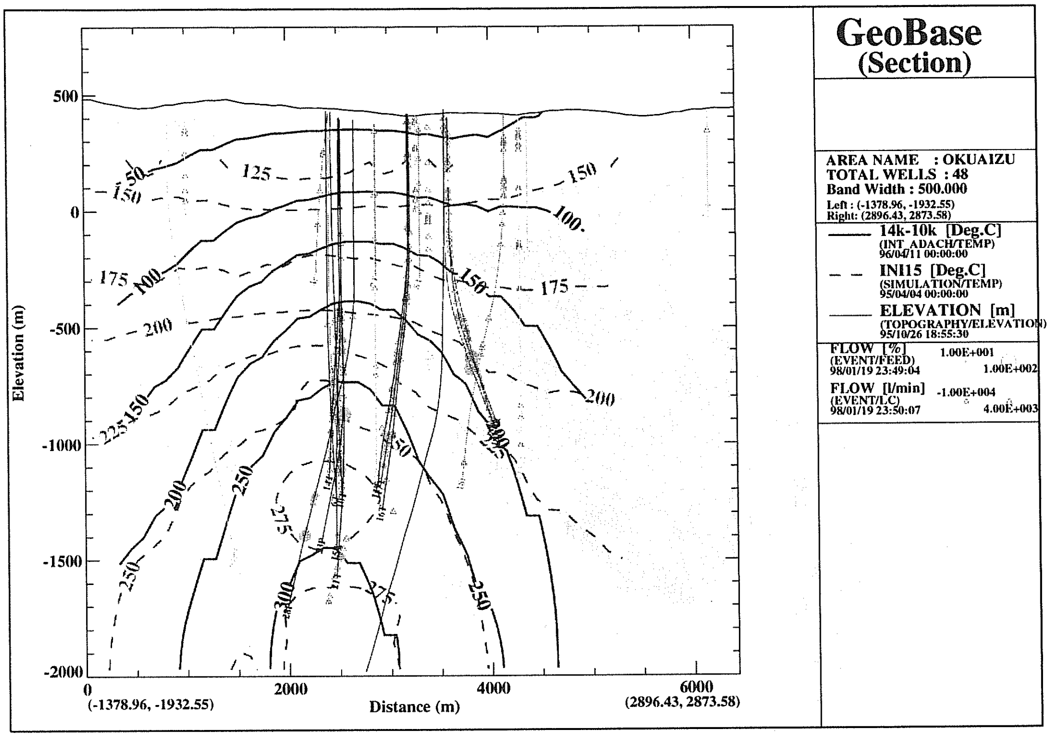

Figure 2. NE-SW cross-sectional view of the underground temperature distribution optimized by steady-state modeling(dash line), and the actual underground temperature distribution (solid line), lost-circulation points (triangle), feed points from PTS logging (circle) and well trajectories (solid line)

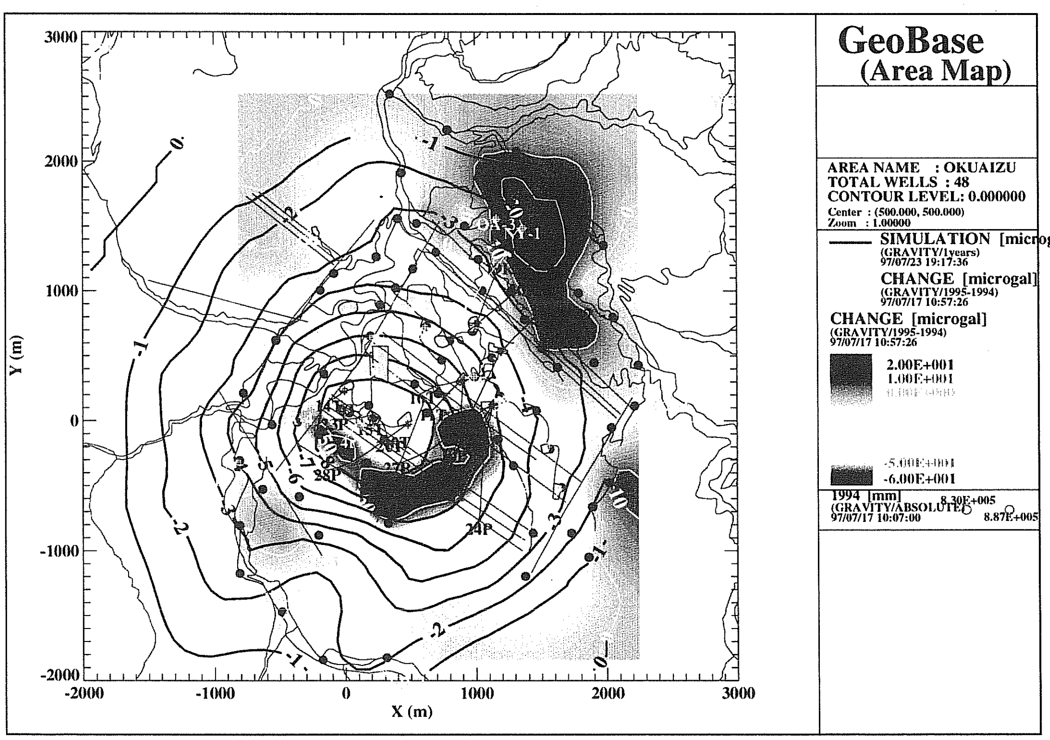

Figure 4 Gravity change predicted one year after the start of production (solid line) and measured values (1995-1994) (filled color & white solid line)

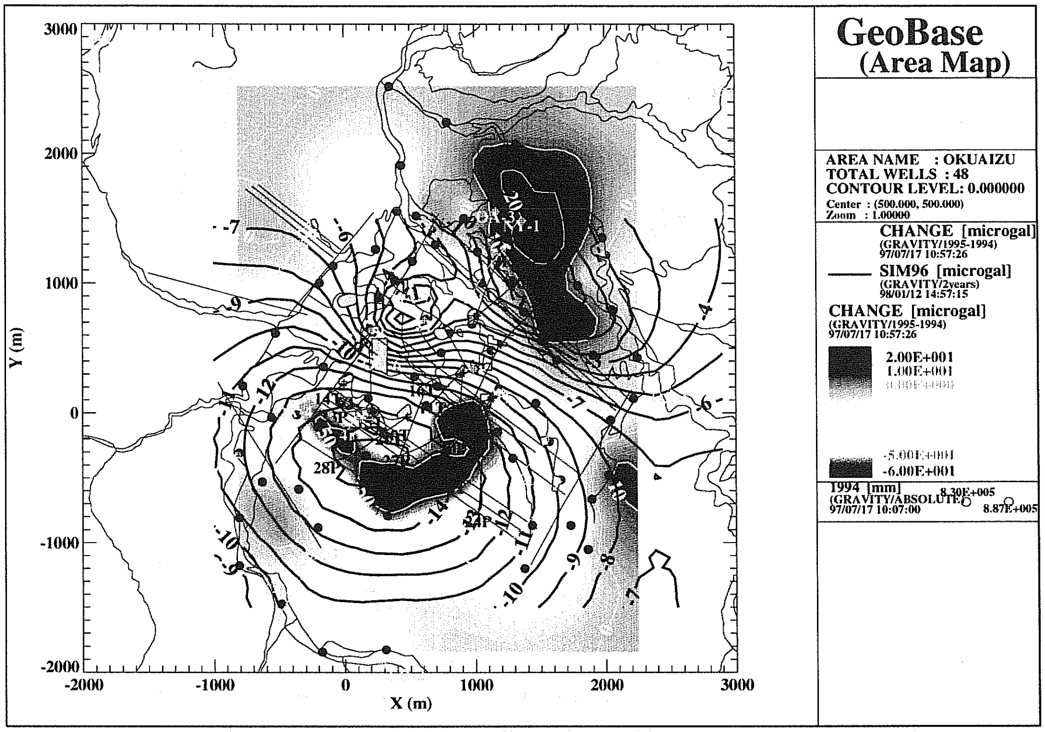

Figure 5 Gravity change predicted one year after the start of production (black solid line) and measured values (1995-1994) (filled color & white solid line) after the production history matching